Atomic force microscope based on vertical silicon probes

Benjamin Walter, Estelle Mairiaux, Marc Faucher

12 June 2017 Volume 110 Number 24

AIP | Applied Physics Letters

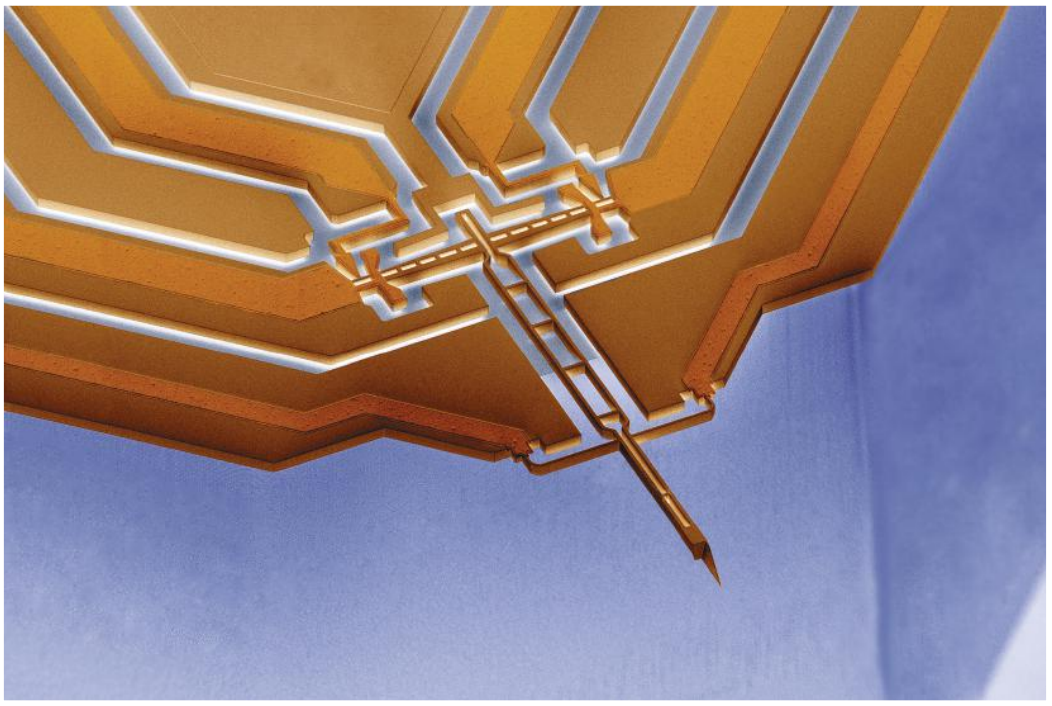

apl.aip.org

Atomic force microscope based on vertical silicon probes

Benjamin Walter,[1] Estelle Mairiaux,[1] and Marc Faucher[1,2]
[1]*Vmicro SAS, Avenue Poincaré, 59650 Villeneuve d'Ascq, France*
[2]*Institut d'Electronique, de Microélectronique et de Nanotechnologie, Univ. Lille, CNRS UMR 8520 - IEMN, F-59000 Lille, France*

(Received 4 March 2017; accepted 24 April 2017; published online 12 June 2017)

A family of silicon micro-sensors for Atomic Force Microscope (AFM) is presented that allows to operate with integrated transducers from medium to high frequencies together with moderate stiffness constants. The sensors are based on Micro-Electro-Mechanical-Systems technology. The vertical design specifically enables a long tip to oscillate perpendicularly to the surface to be imaged. The tip is part of a resonator including quasi-flexural composite beams, and symmetrical transducers that can be used as piezoresistive detector and/or electro-thermal actuator. Two vertical probes (Vprobes) were operated up to 4.3 MHz with stiffness constants 150 N/m to 500 N/m and the capability to oscillate from 10 pm to 90 nm. AFM images of several samples both in amplitude modulation (tapping-mode) and in frequency modulation were obtained. *Published by AIP Publishing.*
[http://dx.doi.org/10.1063/1.4985125]

Since its invention three decades ago,[1] Atomic Force Microscopy (AFM) has rapidly become a standard imaging technique enabling metrology, surface science experiments, and biological studies at the nanoscale.[2,3] AFM is operated by a majority of users in air with setups based on optical beam deflexion (OBD) and cantilever sensors. Although they are improving incrementally, cantilevers remained so far close to the design used in the first technological achievements.[4] Research linked to AFM instrumentation addresses challenges: using multi-frequencies,[5] improving the signal chain,[6] and increasing the imaging speed for monitoring real time dynamic phenomena on surfaces.[7,8] For these objectives, the use of cantilevers face limitations, in particular, when size reduction to access higher resonant frequencies push OBD setups to optical limits. Instrumentation without OBD heads would be desirable, but in the case of self-sensing cantilevers, transducers integration imposes relatively large dimensions that prevent to increase frequencies. Piezoresistive silicon cantilevers[9] were developed in the past for scanning AFM or for information storage,[10,11] but are not as used as passive cantilevers today. Most of the self-sensing probes used today are quartz based. They were developed originally for vacuum or low temperature environments and consist of quartz tuning forks[12] or length extensional resonators.[13] Pioneers of high resolution AFM in vacuum[14] have shown that standard cantilevers with stiffness constants from 2 to 40 N/m (60 kHz to 280 kHz) are not optimal for atomic resolution imaging and suggested to use probes with stiffness constants from 300 N/m to 3000 N/m depending the application, but only the higher value was available up till now with quartz sensors. Silicon Micro-Electro-Mechanical-Systems (MEMS) and Nano-electro-Mechanical-Systems (NEMS) technologies are attractive for exploring probes designs with major concept changes, since they use batch processing that permits large volumes and repeatable probe specifications. Previously, we demonstrated the use of MEMS resonators at very high frequencies[15] that were used in an AFM setup with resonant amplitudes in the range 10–20 pm and stiffness constant above 100 kN/m.[16] Here, we present a family of vertical probes that enable to combine much lower stiffness constants to high amplitude dynamic range, together with low impedance electrical transducers and optimized aspect ratio for the tip. The architecture of these vertical probes (Vprobes) is described in Fig. 1: they are based on a resonator etched in a silicon-on-insulator (SOI) device layer. The resonator includes a tip, itself part of a vertical beam that can move along the Z axis, thanks to four lateral beams extending along the X axis. The structure has been optimized to deliver a resonant mode where the tip moves perpendicularly to the sample, whereas lateral beams experience in-plane flexural motion. To actuate and measure the probe displacement, electro-thermal (ET) and piezoresistive (PR) transducers were integrated on the lateral beams. They both consist of a current injector, a resistive part, and a path to external bonding pads (see Fig. 1). The vertical tip design is

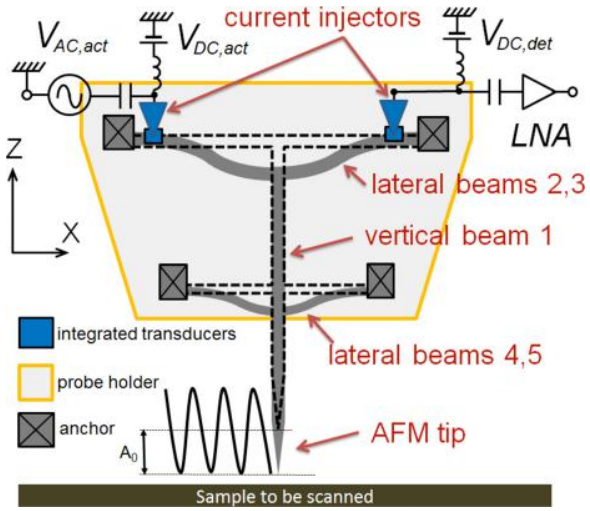

FIG. 1. Principle of the AFM vertical silicon probe (Vprobe) and its resonant mode. The sensor is based on a MEMS resonant body composed of vertical beam 1 and tip that is linked to the substrate though lateral beams 2,3 and 4,5. The AFM tip is monolithically integrated to the vertical structure. The probe also features electro-thermal and piezoresistive transducers located close to the anchors of the upper lateral beams 2,3. Dashed lines denote the resonator at rest.

motivated by imaging samples where mechanical access can be difficult and that require very compact AFM heads. It also intends to lower parasitic effects in AFM electrical or magnetic modes.[17] Our vertical probes were fabricated using specifically developed batch silicon processing steps. We started from commercially available (100) oriented Silicon-On-Insulator (SOI) wafers. Two device layer thicknesses of 0.5 μm (10 Ω cm) and 5 μm (>50 Ω cm) were used. A first lithographic step and plasma etching was done in order to define alignment marks. In a second step, windows were defined to implant boron at a dose of 6×10^{13} at. cm^2, energy 20, and 70 keV, in the intrinsic zone of the transducer. In a third step, other windows were defined and used to implant boron at a dose of 3×10^{15} at. cm^2, energy 20 keV onto the injectors. These two steps take advantage of the flat silicon surface that enables the required submicron alignment and resolution. Then, a lithographic step and Cl_2/BCL_3 plasma etching is used to define the lowest probe part including one of the tip facets, similarly as described in Ref. 11. This step was followed by a low temperature oxide (LTO) deposition. This oxide was patterned and opened according to a rectangular shape, then followed by a tetramethyl ammonium hydroxide (TMAH) etch to produce the second tip facet corresponding to (111) plane [see Fig. 2(c)]. After aluminum contacts were patterned and ohmic contacts were obtained by thermal annealing, the next step consisted in defining the resonator main body including vertical and lateral beams of the double T-shape. Then, the probe holder was defined using Deep Reactive Ion Etching (DRIE) of the silicon handle wafer. Finally, the device was released in vapour-HF etch of the buried oxide. In Fig. 2, we show two Vprobes that are designed according to the architecture of Fig. 1. Vprobe n°1 [Fig. 2(a)] makes use of 5 μm thick SOI, whereas Vprobe n°2 [Fig. 2(b)] makes use of 0.5 μm thick SOI and NEMS design rules. As a practical implementation of the principle shown in Fig. 1, we used composite structures for both lateral and vertical beams. This was done in order to reduce the mass. The obtained tips that are shown in Figs. 2(c) and 2(d) feature typical radii lower than 20 nm, a value comparable to commercial AFM tips.

The transducers' current injectors allow integrating ohmic contacts as close as possible to the resistive part, which reduce the overall resistances. The obtained dipole resistance can thus be kept between 50 and 400 Ω, a very low range that is difficult to reach with out-of-plane MEMS/NEMS cantilevers up till now, owing to the previous state-of-the-art design, doping, and thickness limitations. This low impedance makes the signal interfacing easier with discrete electronics, particularly at MHz frequencies and/or when high cable lengths are necessary. The Vprobe shown in Fig. 2(a) has a 1.18 MHz resonance frequency with 500 N/m stiffness constant, and the Vprobe shown in Fig. 2(b) has a 4.42 MHz resonant frequency with 150 N/m stiffness constant. Depending of their dimensions, the Vprobes have non-vertical modes with lower frequencies than the vertical mode. For Vprobe 1, the lowest mode is at 310 kHz, still a high value in comparison to lateral frequency used for XY scanning, thus not being a limitation for use in fast AFM heads.

After fabrication, the probes were detached from the SOI wafer, glued onto a holder, and transducers pads were electrically connected to the holder coaxial connectors. The probes were characterized using the electrical setup described in Fig. 1, consisting in one bias tee for each transducer, and a low noise amplifier (LNA, model FEMTO HVA-10M-60B). Doppler vibrometry measurements were performed to confirm the in-plane mode nature and provide an amplitude calibration of the signal chain (1.9×10^{-3} V/nm at 1 V detector bias for the Vprobe n°1 shown in Fig. 3(a) shows resonance spectra

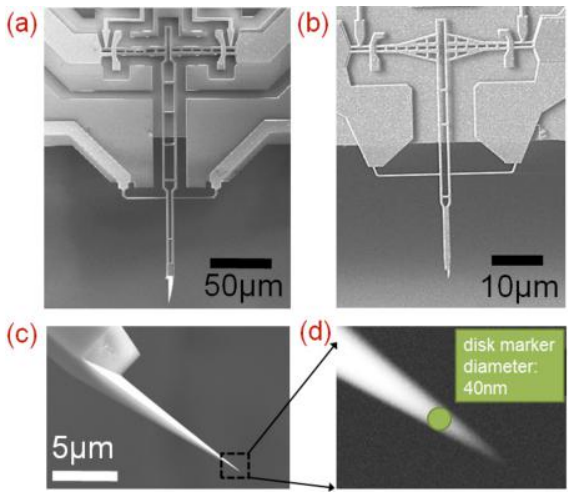

FIG. 2. SEM images of two micro-fabricated Vprobes. (a) Vprobe n°1 made on 5 μm device layer SOI wafer: operating frequency 1.18 MHz, stiffness 500 N/m. On this probe, the tip has an electrical access, thanks to metal lines deposited onto lateral beams 4,5. (b) More miniaturized device Vprobe n°2 made on 500 nm thick SOI: operating frequency 4.3 MHz, 150 N/m. (c) Integrated high aspect ratio silicon tip obtained on Vprobe 1, and (d) zoom at the tip apex.

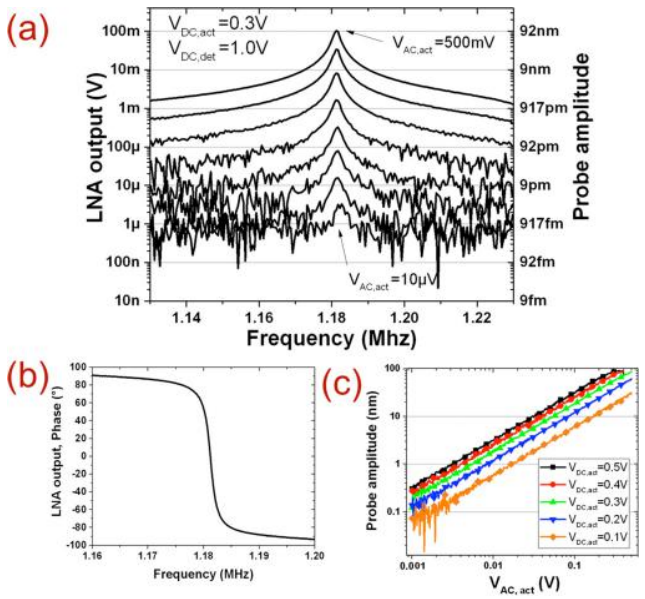

FIG. 3. Electro-mechanical characterization of a Vprobe n°1. (a) Left Y-axis: probe resonance signal taken from the piezoresistive transducer at constant bias of 0.3 V at the actuator and 1 V at detector; right Y: corresponding amplitude derived from optical calibration. The different curves correspond to AC voltage from 10 μV to 0.5 V applied to the actuator. (b) Typical phase spectrum of Vprobe 1. (c) Optical calibration of the mechanical amplitude versus DC and AC voltages fed to the ET actuator.

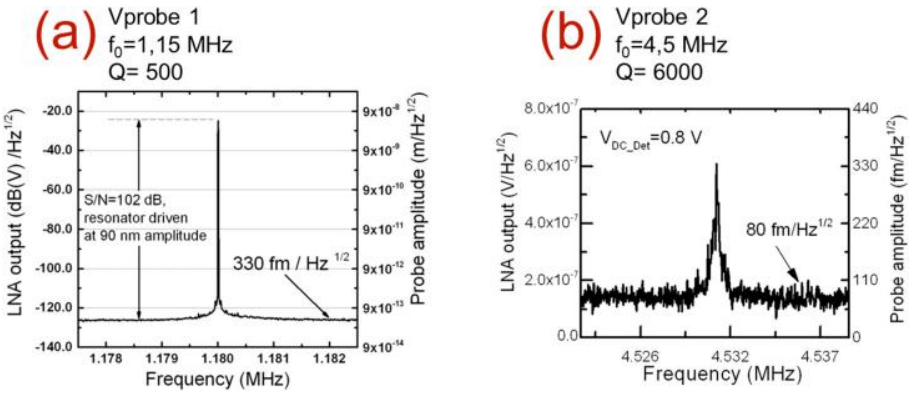

FIG. 4. (a) Signal to noise ratio obtained on a Vprobe n°1. (b) Thermal noise analysis performed on a Vprobe n°2. The limits of detection given by the noise floor outside the resonance are 330 fm/Hz$^{1/2}$ for Vprobe 1 and 80 fm/Hz$^{1/2}$ for Vprobe 2.

proving that the ET transducer enables actuation from 20 pm to 90 nm without generation of artifacts known in ceramic-based bulk actuation in OBD AFM heads. This quality of harmonic excitation is also seen on the phase spectrum shown in Fig. 3(b). Figure 3(c) shows the probe amplitude at resonance versus the AC power and also the dependence with DC bias applied on the actuator. The large amplitude range will enable to use Vprobes both in tapping mode AFM and in dynamic modes requiring lower amplitudes (non-contact AFM). The non-vertical component of the motion at the same frequency was measured and represents 6% of the vertical amplitude.

We conducted on the Vprobes a first Noise and SNR study that is presented in Fig. 4. Driven at an amplitude of 90 nm, Vprobe 1 output enables a 102 dB SNR. Thanks to the calibration procedure, we deduce that the floor corresponds to a detector noise density of 330 fm/Hz$^{1/2}$. On a Vprobe n°2, the noise achieved noise density is 80 fm/Hz$^{1/2}$ and the thermal noise is more easily seen [Fig. 4(b)]. We attribute this behavior to the different doping profiles: on Vprobe n°1, the implantation depth is limited to 0.3 μm, whereas most of the 0.5 μm thick device layer is implanted in the case of Vprobe n°2, thus maximizing the piezoresistive signal. The detector noise density is here comparable to standard OBD setups.[18,19] Further design refinements and also process improvements are feasible to improve the signal to noise ratio.

Finally, the first AFM in air with the Vprobes was implemented on a modified commercial microscope (multimode AFM, Bruker) where head optical parts were removed. A SiC surface was imaged in frequency modulation mode using a Vprobe n°2 (Fig. 5), were the vicinal steps were clearly seen. Figure 5(a) shows an image made with Vprobe n°1 of a polymer sample polystyrene and polyolefin elastomer (PS-LDPE-12M, bruker). The image is obtained in amplitude modulation (AM-AFM) with 20 nm amplitude. Figure 6(a) is the topography, and Fig. 6(b) shows strong phase contrast: in the context of polymers mechanical properties characterization with AFM,[20,21] this preliminary result opens the path to viscoelastic studies with the capability of high amplitudes combined to high frequencies. Finally, Fig. 7 shows an image of DNA on mica sample using a Vprobe n°1 in frequency modulation mode. Here, the linear speed is 8 μm/s, and the accuracy of topographic imaging across a larger scan size implying the stability of probe signal on longer timescale is thus assessed in real conditions.

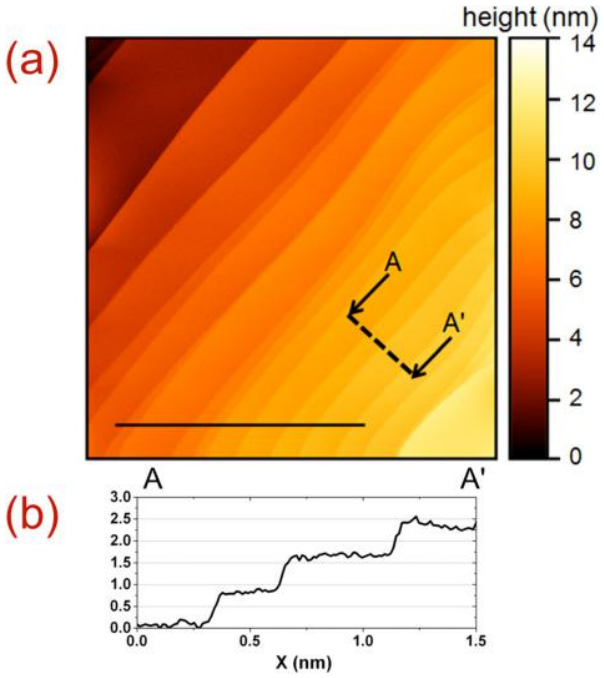

FIG. 5. (a) First image obtained on SiC surface (scan size 6.5 × 6.5 μm, scale bar 4 μm. 512points × 512 lines, sample "SiC/0.75" from ND-MDT company). The Vprobe n°2 is operated with f = 4.3 MHz, Q = 180 in air, k = 150 N/m, and imaging speed 10 μm/s. FM-AFM mode is used in repulsive mode with 30 nm amplitude and 20 Hz setpoint. (b) Height profile showing the 0.75 nm steps.

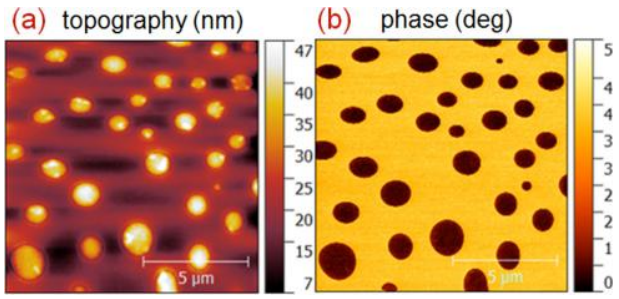

FIG. 6. Amplitude Modulation (AM-AFM) imaging with Vprobe n°1 of a polymer sample polystyrene and polyolefin elastomer (512 points × 512 lines). (a) is the topographic image, and (b) represents the phase signal. Imaging parameters: frequency 1.2 MHz, stiffness constant 500 N/m, Q = 600, free amplitude A0 = 20 nm, amplitude setpoint A1 = 19.8 nm, and scanning speed 10 μm/s.

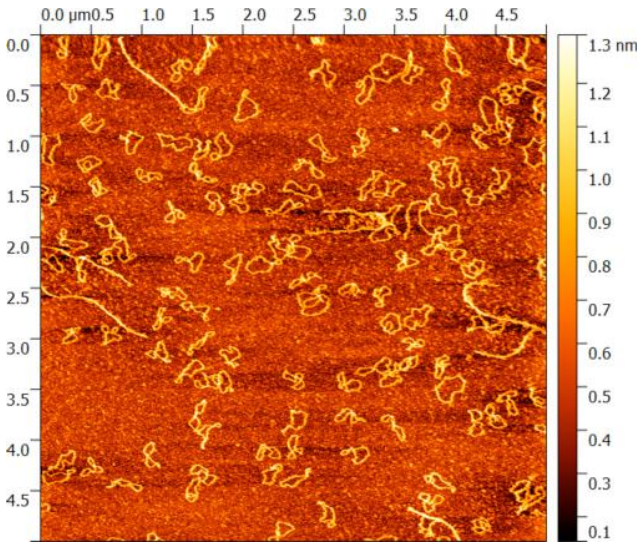

FIG. 7. 512 points × 512 lines topographic DNA imaging in FM-AFM mode using a Vprobe n°1. FM-AFM mode is used in repulsive mode with 24 nm amplitude, quality factor Q = 600, and 75 Hz setpoint. Imaging speed is 8 μm/s.

In conclusion, we introduced vertical batch fabricated silicon probes were MEMs resonator engineering proves robust for having long tips with well-defined vertical motion. The design of integrated transducers enables a wide range of operating amplitudes in dynamic mode and low impedance signal chain at high frequencies. This technology offers strong perspectives for several AFM setups requiring high scanning speed, ultrahigh vacuum and/or low temperatures. Moreover, different setups requiring very compact heads, specific mechanical or optical access should benefit from this technology.

The authors wish to thank the IEMN staff for fruitful interaction. Technological work was performed at IEMN clean room, part of the RENATECH network.

[1]G. Binnig, C. F. Quate, and C. Gerber, Phys. Rev. Lett. **56**(9), 930 (1986).
[2]F. J. Giessibl, Rev. Mod. Phys. **75**(3), 949 (2003); T. R. Albrecht and C. F. Quate, J. Appl. Phys. **62**(7), 2599 (1987).
[3]P. Parot, Y. F. Dufrêne, P. Hinterdorfer, C. Le Grimellec, D. Navajas, J.-L. Pellequer, and S. Scheuring, J. Mol. Recognit. **20**(6), 418 (2007).
[4]T. R. Albrecht, S. Akamine, T. E. Carver, and C. F. Quate, J. Vac. Sci. Technol., A **8**(4), 3386 (1990).
[5]A. P. Nievergelt, J. D. Adams, P. D. Odermatt, and G. E. Fantner, Beilstein J. Nanotechnol. **5**, 2459 (2014).
[6]M. G. Ruppert, D. M. Harcombe, and S. O. R. Moheimani, IEEE/ASME Trans. Mechatronics **21**(6), 2705 (2016).
[7]A. Toshio, K. Noriyuki, T. Eisuke, M. Daisuke, S. Kiwamu, and T. Akitoshi, Proc. Nat. Acad. Sci. U. S. A. **98**(22), 12468 (2001).
[8]H. Watanabe, T. Uchihashi, T. Kobashi, M. Shibata, J. Nishiyama, R. Yasuda, and T. Ando, Rev. Sci. Instrum. **84**(5), 053702 (2013).
[9]M. Tortonese, R. C. Barrett, and C. F. Quate, Appl. Phys. Lett. **62**(8), 834 (1993).
[10]W. P. King, T. W. Kenny, K. E. Goodson, G. L. W. Cross, M. Despont, U. T. Durig, H. Rothuizen, G. Binnig, and P. Vettiger, J. Microelectromech. Syst. **11**(6), 765 (2002).
[11]R. P. Ried, H. Jonathon Mamin, B. D. Terris, L.-S. Fan, and D. Rugar, J. Microelectromech. Syst. **6**(4), 294 (1997).
[12]F. J. Giessibl, Appl. Phys. Lett. **76**(11), 1470 (2000).
[13]T. An, T. Nishio, T. Eguchi, M. Ono, A. Nomura, K. Akiyama, and Y. Hasegawa, Rev. Sci. Instrum. **79**(3), 033703 (2008).
[14]F. J. Giessibl, H. Bielefeldt, S. Hembacher, and J. Mannhart, Appl. Surf. Sci. **140**(3), 352 (1999).
[15]M. Faucher, B. Walter, A. S. Rollier, K. Seguini, B. Legrand, G. Couturier, J. P. Aime, C. Bernard, R. Boisgard, and L. Buchaillot, paper presented at The TRANSDUCERS 2007 - 2007 International Solid-State Sensors, Actuators and Microsystems Conference, 2007.
[16]S. Houmadi, B. Legrand, J. P. Salvetat, B. Walter, E. Mairiaux, J. P. Aimé, D. Ducatteau, P. Merzeau, L. Buisson, J. Elezgaray, D. Théron, and M. Faucher, paper presented at The 2015 28th IEEE International Conference on Micro Electro Mechanical Systems (MEMS), 2015.
[17]G. Elias, T. Glatzel, E. Meyer, A. Schwarzman, A. Boag, and Y. Rosenwaks, Beilstein J. Nanotechnol. **2**, 252 (2011).
[18]S. Morita, F. J. Giessibl, E. Meyer, and R. Wiesendanger, Noncontact Atomic Force Microscopy (Springer editions), Vol. 3.
[19]M. Dukic, J. D. Adams, and G. E. Fantner, Sci. Rep. **5**, 16393 (2015).
[20]S. Shi, D. Guo, and J. Luo, RSC Adv. **7**(19), 11768 (2017).
[21]O. Sahin and N. Erina, Nanotechnology **19**(44), 445717 (2008).